Journal of Advanced Ceramics
2021, **10**(6): 1291–1298
https://doi.org/10.1007/s40145-021-0504-z

ISSN 2226-4108
CN 10-1154/TQ

Research Article

In-situ growth of MAX phase coatings on carbonised wood and their terahertz shielding properties

Jiaxuan HUANG[a,b,c], Hujie WAN[d], Mian LI[b,c], Yiming ZHANG[b,c], Jianfeng ZHU[a,*], Xuelin LI[a], Wenchao SHUI[d], Yao LI[d], Xiaomeng FAN[e], Qiye WEN[d,*], Xu XIAO[d,*], Qing HUANG[b,c,*]

[a]*School of Shaanxi University of Science and Technology, Xi'an 710021, China*
[b]*Engineering Laboratory of Advanced Energy Materials, Ningbo Institute of Materials Technology and Engineering, Chinese Academy of Sciences, Ningbo 315201, China*
[c]*Qianwan Institute of CNiTECH, Zhongchuangyi Road, Hangzhou Bay District, Ningbo 315336, China*
[d]*School of Electronic Science and Engineering, State Key Laboratory of Electronic Thin Film and Integrated Devices, University of Electronic Science and Technology of China, Chengdu 610054, China*
[e]*State Key Laboratory of Solidification Processing, School of Materials Science and Engineering, Northwestern Polytechnical University, Xi'an 710072, China*

Received: March 24, 2021; Revised: April 29, 2021; Accepted: June 1, 2021

Abstract: Electromagnetic interference (EMI) shielding materials have received considerable attention in recent years. The EMI shielding effectiveness (SE) of materials depends on not only their composition but also their microstructures. Among various microstructure prototypes, porous structures provide the advantages of low density and high terahertz wave absorption. In this study, by using carbonised wood (CW) as a template, 1-mm-thick MAX@CW composites (Ti_2AlC@CW, V_2AlC@CW, and Cr_2AlC@CW) with a porous structure were fabricated through the molten salt method. The MAX@CW composites led to the formation of a conductive network and multilayer interface, which resulted in improved EMI SE. The average EMI SE values of the three MAX@CW composites were > 45 dB in the frequency of 0.6–1.6 THz. Among the composites, V_2AlC@CW exhibited the highest average EMI SE of 55 dB.

Keywords: MAX phases; biomimics; electromagnetic interference (EMI); terahertz shielding

* Corresponding authors.
E-mail: J. Zhu, zhujf@sust.edu.cn;
Q. Wen, qywen@uestc.edu.cn;
X. Xiao, xuxiao@uestc.edu.cn;
Q. Huang, huangqing@nimte.ac.cn

1 Introduction

With the rapid development of terahertz (THz) technology, especially the use of THz band as the next-generation (6G) communication band, THz shielding materials are urgently required to prevent electronic device malfunctions resulting from signal crosstalk and to protect people from electromagnetic pollution. Moreover, the development of lightweight and environment-friendly THz shielding materials is preferred [1–4]. Typically, the effectiveness of THz shielding materials is highly related to their microstructures [5,6]. For example, structures with specific interface contacts (such as core–shell, sandwich-like, and porous foam structures) can be used to induce interfacial polarisation to dissipate THz waves, and thus, to improve electromagnetic interference shielding effectiveness (EMI SE) [7–11]. Among shielding materials, materials with porous structures have attracted considerable attention due to their special structure, large specific surface area, and light weight.

As a porous material, carbonised wood (CW) obtained through the high-temperature carbonisation of natural wood is widely studied because of its light weight, multistage pore structure, and anisotropy [12–16]. The natural three-dimensional (3D) porous conductive network of CW renders it a promising candidate for high-effectiveness EMI shielding [17–20]. However, the single-shielding mechanism of CW limits its EMI shielding potential. Therefore, various conductive materials are integrated into a CW template to obtain functional composites with an improved EMI SE [21].

Therefore, in this study, we used CW as the template to design a wood-based conductive composite with a 3D porous structure as a THz shielding material. MAX (Ti_2AlC, V_2AlC, and Cr_2AlC) phases are a family of layered ternary transition metal carbides/nitrides, which exhibit ceramic and metallic attributes, such as superior oxidation and corrosion resistance, eminent electrical/thermal conductivity, and high dielectric loss. Therefore, MAX phases are proposed as ideal EMI shielding materials in harsh environments [22–24]. In this study, a MAX@CW composite (Ti_2AlC@CW, V_2AlC@CW, and Cr_2AlC@CW) with a porous structure was fabricated through the *in-situ* growth of MAX phase coatings on CW in a molten salt bath. The MAX@CW composites retained the porous structure characteristics of the CW template. Meanwhile, the CW template guides the directional assembly of the MAX phase by making it filling into the porous structure of the CW, showing a multi-interface. This unique structure of the MAX@CW composites provided paths for the dissipation of THz waves within the porous network structure. This dissipation led to a considerable increase in transmission loss and the improvement of EMI SE. Thus, the MAX@CW composites exhibit a considerably higher SE than CW and can be used as a highly effective EMI shielding material.

2 Experimental

2. 1 Synthesis of CW

First, natural linden wood was cut into pieces of dimensions 2.5 cm × 3.5 cm × 3 mm. These pieces were placed into an alumina crucible, and high-temperature carbonisation was performed at 1000 ℃ for 6 h in an argon atmosphere. The temperature was increased from room temperature to 1000 ℃ at a rate of 4 ℃/min. The carbonised wood slices were carefully polished with a 1000-mesh sand tray to obtain 1-mm-thick CW pieces. Subsequently, carbon debris that has been polished was removed after several rounds of ultrasonic washing with deionised water and ethanol. Finally, the pieces were dried in an ordinary oven to obtain the final CW samples.

2. 2 Synthesis of MAX@CW

The MAX@CW composites were prepared using the molten salt method. CW was used both as the template and carbon source. The M-site metal powder (Ti, V, and Cr) and A-site metal powder (Al) with the particle size of approximately 1 μm were used as raw materials to synthesize the target MAX@CW. Furthermore, analytical grade NaCl/KCl purchased from Shanghai Aladdin Industrial Co., Ltd., China, was selected for the molten salt bath.

The MAX@CW composites were prepared *in-situ* on a porous CW matrix in the salt bath as follows: First, the staring materials were mixed in a molar ratio of M-site (i.e., Ti, V, and Cr): Al : CW : NaCl : KCl = 2 : 1.2 : 0.8 : 4 : 4 to cover CW completely. Next, the mixed materials were placed in an alumina crucible and packaged in a tube furnace. The tube furnace was heated from room temperature to 800 ℃ at the rate of 4 ℃/min under argon atmosphere, and this temperature was maintained for 3 h. The furnace was then heated to

a sintering temperature at the rate of 4 ℃/min for 3 h (the sintering temperatures for Ti_2AlC@CW, V_2AlC@CW, and Cr_2AlC@CW were 1100, 1100, and 900 ℃, respectively). Subsequently, the tube furnace was cooled to room temperature at the rate of 4 ℃/min. Next, the product was washed many times with deionised water at room temperature to remove salt. Finally, the MAX@CW composites were obtained after drying.

2. 3 Characterisation

The derived samples were analysed using a Bruker D8 Discovery X-ray diffractometer (irradiated by Cu Kα, λ = 1.5406 Å), with the acceleration voltage of 40 kV, filament current of 40 mA, and 2θ range of 10°–70° at a step size of 0.02°. The structure and vibration characteristics of CW and MAX@CW were analysed using a confocal Raman microscope (Renishaw Invia Reflex, UK) with an excitation wavelength of 532 nm. A scanning electron microscope (Quanta FEG 250, FEI, USA) was used to characterise the morphology and microstructure of the CW and MAX@CW composites. The electrical conductivity of the material was measured using a four-probe detector (Cresbox, Napson, Japan). Terahertz time-domain spectroscopy (THZ-TDS) was employed at room temperature (22 ℃) and a humidity of 5% (FiCO, USA). The total spectral range was 0.2–3.0 THz (effective spectrum range: 0.3–1.65 THz), with a repetition frequency of 1 kHz, and the dimensions of the samples tested were 2 cm × 3 cm × 1 mm.

3 Results and discussion

3. 1 Material characterisation

The composition of CW and MAX@CW was confirmed through X-ray diffraction (XRD) and Raman spectra. CW exhibits two wide diffraction peaks at approximately 23° and 44°, which denote that the obtained CW is amorphous (Fig. 1(a)) [25]. For the MAX@CW samples, the peaks of CW disappeared and the diffraction peaks of Ti_2AlC, V_2AlC, and Cr_2AlC appeared, indicating the formation of corresponding MAX phase coatings. The Raman spectra are highly sensitive to the surface change of materials, and thus, can be used to detect the formation of CW and MAX@CW. CW shows two strong characteristic peaks near 1350 and 1600 cm^{-1}, which represent the D and G peaks of carbon, respectively (Fig. 1(b)) [26]. For the Ti_2AlC@CW sample, the peaks at 260–270 and 360 cm^{-1} correspond to the ω_2, ω_3, and ω_4 vibration modes of Ti_2AlC, indicating the formation of Ti_2AlC. For V_2AlC@CW and Cr_2AlC@CW, the characteristic peaks of V_2AlC and Cr_2AlC were detected, which confirmed their composition [27,28].

Figure 2(a) schematically illustrates the fabrication of the MAX@CW composites. The process is a two-step synthesis. In the first step, porous structure CW is prepared by carbonising natural linden wood at high temperature. In the next step, MAX phase coatings are grown *in-situ* on the CW template through a high-temperature molten salt reaction. The metallic elements existing in an ionic form in the molten salt media can infiltrate into the pores of CW and react with the carbon matrix to form the MAX phases, which is driven by the pressure difference between the inside and outside of CW pores (i.e., the capillary effect) [29,30].

Figure 2(b) presents the optical photograph of the product. The colour of CW is black, and MAX@CW exhibits a metallic lustre, indicating that the MAX phases are successfully coated on the carbonised wood substrate. CW has a rich pore structure because linden is a natural organic polymer compound, mainly composed of cellulose, hemicellulose, and lignin (Figs. 2(c)–2(f)).

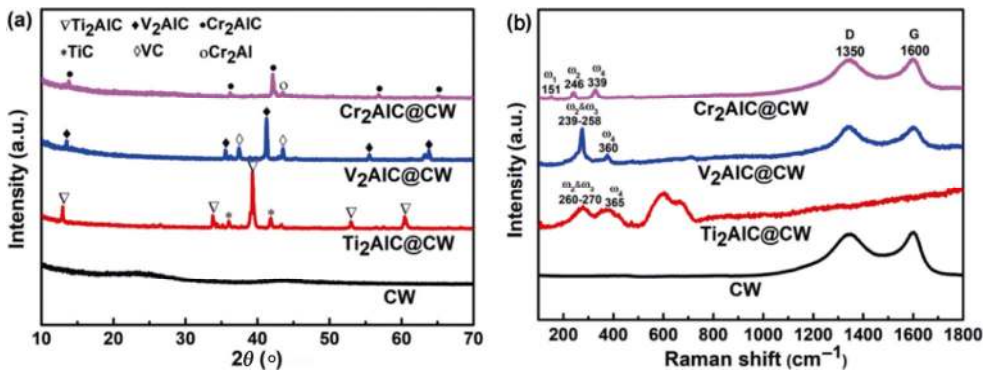

Fig. 1 (a) X-ray diffraction (XRD) patterns and (b) Raman spectra of CW and MAX@CW.

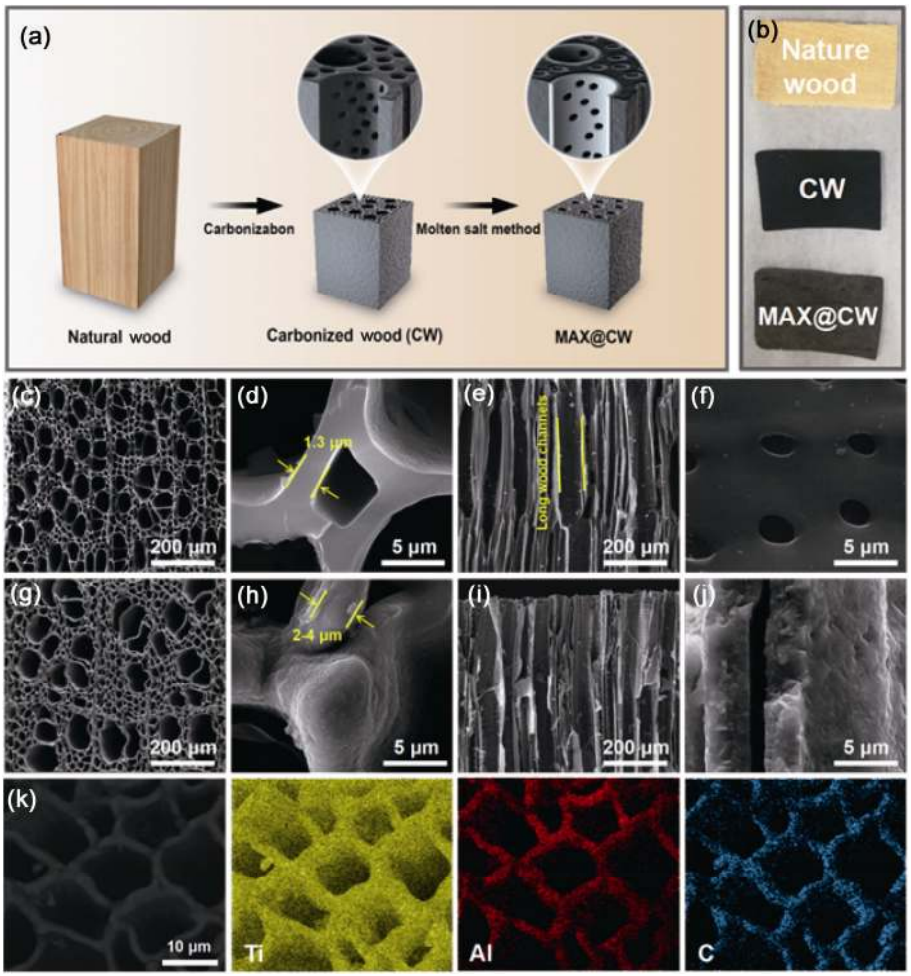

Fig. 2 Schematic of the fabrication process and macro- and micro-structure of the samples. (a) Schematic of the fabrication process. (b) Optical photos of natural wood, CW, and MAX@CW. (c–f) Scanning electron microscopy (SEM) images of bare CW. (g–j) SEM images of Ti_2AlC@CW. (k) X-ray surface scanning of Ti_2AlC@CW.

These substances further decompose and evaporate during high-temperature carbonisation, resulting in a honeycomb pore structure of various length scales ranging from nanometer to micron. The CW pores were mainly oval, with large and small pores of 30–60 and 10−15 μm, respectively. The channels of CW are long and straight, which is favourable for the impregnation of the MAX phase coating (Figs. 2(e) and 2(f)). Because the microstructure of Ti_2AlC@CW, V_2AlC@CW, and Cr_2AlC@CW is similar, we selected Ti_2AlC@CW as a representative composite to show their microstructure. Because of the atomic-level reaction in molten salt, Ti_2AlC@CW exhibits the natural porous structure of CW without morphological distortion or pore blockage (Figs. 2(g)–2(j)). Furthermore, Figs. 2(g)–2(h) show that the surface of MAX@CW samples differs from that of the smooth CW substrate. MAX@CW with this porous structure exhibits numerous surfaces and interfaces, which can lead to an increase in the transmission path of incident electromagnetic waves, resulting in multiple scattering, and an increase in electromagnetic wave attenuation.

3. 2 EMI SE measurements

Typically, materials with large electrical conductivity are required to obtain high EMI SE values. Figure 3(a) illustrates the electrical conductivity of CW and three MAX@CW composites (Ti_2AlC@CW, V_2AlC@CW, and Cr_2AlC@CW). The results revealed that the electrical conductivity of the three MAX@CW composites was higher than that of CW, and V_2AlC@CW exhibited the highest conductivity. The high conductivity of MAX@CW is mainly realised by free electron carriers provided by the MAX phase particles. When the concentration of the MAX phases reaches a certain critical value, the MAX phases in the system line up to form a conductive

infinite network chain. The "queue" of the conductive phase acts as a bridge, causing the free electron carriers to pass through the bridge from one end to the other, thus improving its conductivity. Furthermore, the interface effect between CW and MAX phase coatings in MAX@CW contributes to the formation of efficient conductive networks in MAX@CW [31].

To investigate the EMI SE of CW and MAX@CW, we compared the SE of 1 mm CW and the three MAX@CW composites (Fig. 3(b)). The three MAX@CW composites exhibited an SE of > 45 dB, which was considerably higher than that of CW (~42 dB), in the frequency range of 0.6–1.6 THz. Among the composites, V_2AlC@CW with the highest electrical conductivity exhibited the the highest EMI SE value of approximately 55 dB. This phenomenon occurred because the conductor material can reflect and guide THz waves, and then, produce current or magnetic polarisation opposite to the source electromagnetic field in the conductor, thus leading to a decrease in the radiation effect of the source electromagnetic field. Therefore, the energy of THz waves attenuates rapidly in an excellent conductor. Furthermore, the increased conductivity can result in a higher impedance mismatch between the free space and MAX@CW interface, which can contribute to higher internal multiple reflection and lead to an increase in its EMI SE [32]. Moreover, when THz waves enter the MAX@CW composites, the higher conductivity leads to a larger eddy current, which converts THz wave energy into Joule heat, thus improving the absorption loss of THz waves [33]. Because of numerous interfaces between the CW and MAX phases in MAX@CW, effective interface polarisation can be induced, which improves the dissipation of THz wave energy. Therefore, the MAX@CW composites exhibited enhanced EMI SE compared to CW, and V_2AlC@CW exhibited the highest SE value.

The dominant shielding mechanism of CW is the THz wave absorption. The average absorption coefficient of CW is 79% and reflection coefficient is 21%. And the average absorption coefficients of Ti_2AlC@CW, V_2AlC@CW, and Cr_2AlC@CW are 36%, 23%, and 42%, respectively. By contrast, Ti_2AlC@CW, V_2AlC@CW, and Cr_2AlC@CW exhibit high reflection coefficients of 64%, 77%, and 58%, respectively (Figs. 3(c) and 3(d)). Shielding due to reflection was the dominant mechanism in the three MAX@CW composites. The change in the shielding mechanism can be understood from several proposed mechanisms (Fig. 4). When the THz waves are incident on the CW surface, the impedance mismatch decreases because CW has a large open hole. In this case, the incident THz waves can easily enter the channel structure of CW with low reflection, which results in high

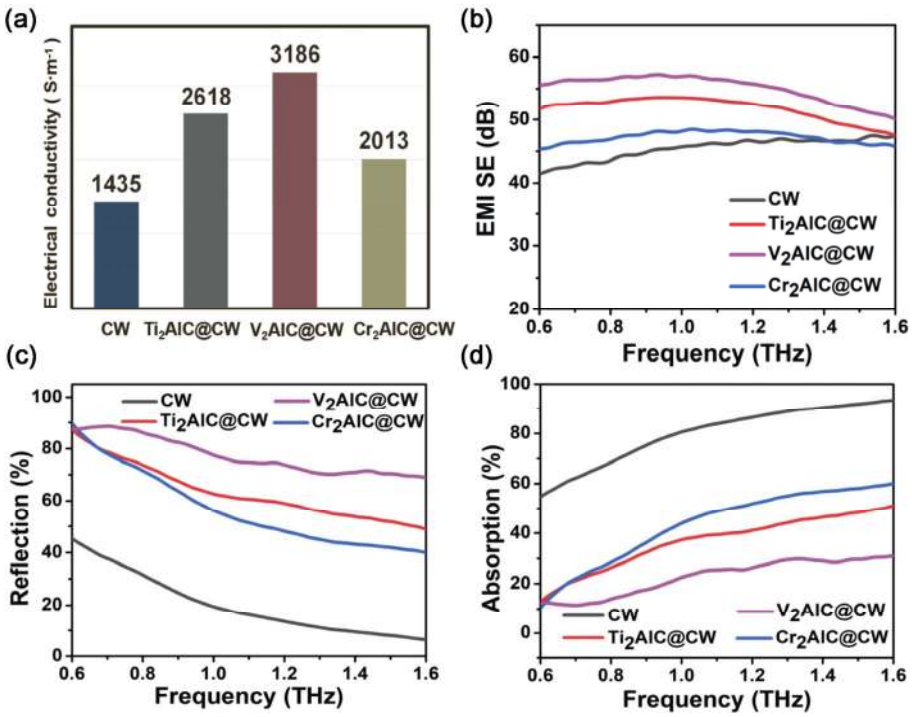

Fig. 3 Electrical conductivity and EMI SE of CW and MAX@CW of 1 mm in thickness in the perpendicular channel direction. (a) Conductivity of CW and MAX@CW. (b) Total EMI SE of CW and MAX@CW. (c) Reflection of CW and MAX@CW. (d) Absorption of CW and MAX@CW.

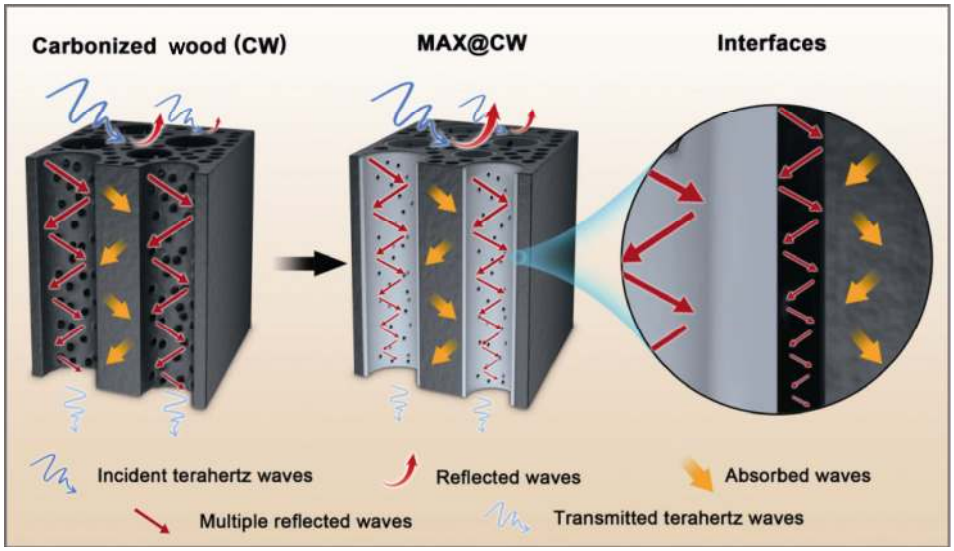

Fig. 4 Morphological structure and THz shielding mechanism of CW and MAX@CW.

absorption. Thus, many THz waves are absorbed and subsequently attenuated [34]. The MAX@CW composites mainly reflect THz waves. The mechanism can be explained as follows: When THz waves strike the surface of a MAX@CW composite, these waves interact strongly with a high electron density of MAX-phase coatings on the surface, resulting in a decrease in energy of the THz waves through the immediate reflection of THz waves. Furthermore, the numerous interfaces between CW and the MAX phase in the MAX@CW composites can induce effective interface polarisation, thereby enhancing the loss ability of the THz waves. In addition, the surviving THz waves enter the channel of MAX@CW, thus traversing through a long transmission path, which causes further energy dissipation of THz waves after multiple reflections inside the channel [35,36]. This phenomenon is in stark contrast to pure CW, which has only a single interface and no interlayer reflecting surfaces to provide multiple internal reflection phenomenon.

4 Conclusions

MAX@CW composites were prepared on CW templates through the *in-situ* reaction in the molten salt bath. The as-obtained MAX@CW composites inherit the specific microstructure of the CW template, exhibiting a 3D interpenetrating pore structure and high specific surface area. MAX@CW with the porous structure causes the formation of a continuous conductive network structure, which can lead to an increase in the transmission paths for incident THz waves, thereby achieving multiple reflections and increasing electromagnetic wave attenuation. Therefore, MAX@CW exhibits excellent electromagnetic shielding performance in the THz band. In the frequency of 0.6–1.6 THz, the total electromagnetic SE of the three MAX@CW composites is > 45 dB, and the V_2AlC@CW exhibits the highest EMI SE of 55 dB. The results indicated the potential of developing functional materials by using natural biological structures as templates.

Acknowledgements

This study was supported financially by the National Natural Science Foundation of China (Grant Nos. 51902320, 61831012, and U2004212). Qing Huang thanks International Partnership Program of Chinese Academy of Sciences (Grant No. 174433KYSB20190019), the Leading Innovative and Entrepreneur Team Introduction Program of Zhejiang (Grant No. 2019R01003). Mian Li acknowledges the support from the fund of the State Key Laboratory of Solidification Processing in NPU (Grant No. SKLSP201917).

References

[1] Shahzad F, Alhabeb M, Hatter CB, *et al*. Electromagnetic interference shielding with 2D transition metal carbides (MXenes). *Science* 2016, **353**: 1137–1140.

[2] Amin M, Siddiqui O, Abutarboush H, *et al*. A THz graphene metasurface for polarization selective virus sensing. *Carbon* 2021, **176**: 580–591.

[3] Cheng KB, Ramakrishna S, Lee KC. Electromagnetic

shielding effectiveness of copper/glass fiber knitted fabric reinforced polypropylene composites. *Compos A*: *Appl Sci Manuf* 2000, **31**: 1039–1045.

[4] Tian MW, Du MZ, Qu LJ, *et al*. Electromagnetic interference shielding cotton fabrics with high electrical conductivity and electrical heating behavior via layer-by-layer self-assembly route. *RSC Adv* 2017, **7**: 42641–42652.

[5] Zhao HB, Cheng JB, Wang YZ. Biomass-derived Co@ crystalline carbon@carbon aerogel composite with enhanced thermal stability and strong microwave absorption performance. *J Alloys Compd* 2018, **736**: 71–79.

[6] Xia T, Zhang C, Oyler NA, *et al*. Hydrogenated TiO_2 nanocrystals: A novel microwave absorbing material. *Adv Mater* 2013, **25**: 6905–6910.

[7] Han M, Yin X, Li X, *et al*. Laminated and two-dimensional carbon-supported microwave absorbers derived from MXenes. *ACS Appl Mater Interfaces* 2017, **9**: 20038–20045.

[8] Ohlan A, Singh K, Chandra A, *et al*. Microwave absorption behavior of core–shell structured poly (3,4-ethylenedioxy thiophene)–barium ferrite nanocomposites. *ACS Appl Mater Interfaces* 2010, **2**: 927–933.

[9] Han MK, Yin XW, Kong L, *et al*. Graphene-wrapped ZnO hollow spheres with enhanced electromagnetic wave absorption properties. *J Mater Chem A* 2014, **2**: 16403–16409.

[10] Zeng Q, Xu DW, Chen P, *et al*. 3D graphene-Ni microspheres with excellent microwave absorption and corrosion resistance properties. *J Mater Sci*: *Mater Electron* 2018, **29**: 2421–2433.

[11] Zhang WJ, Zhang ZD, Jiang YL, *et al*. Porous Fe@Fe_3O_4–C nanocomposite using polyvinyl alcohol sponge as template for microwave absorption. *J Electron Mater* 2020, **49**: 6394–6402.

[12] Song JW, Chen CJ, Zhu SZ, *et al*. Processing bulk natural wood into a high-performance structural material. *Nature* 2018, **554**: 224–228.

[13] Chen FJ, Gong AS, Zhu MW, *et al*. Mesoporous, three-dimensional wood membrane decorated with nanoparticles for highly efficient water treatment. *ACS Nano* 2017, **11**: 4275–4282.

[14] Kurosaki F, Ishimaru K, Hata T, *et al*. Microstructure of wood charcoal prepared by flash heating. *Carbon* 2003, **41**: 3057–3062.

[15] Shibata K, Okabe T, Saito K, *et al*. Electromagnetic shielding properties of woodceramics made from wastepaper. *J Porous Mater* 1997, **4**: 269–275.

[16] Vartapetyan RS, Voloshchuk AM, Buryak AK, *et al*. Water vapor adsorption on chars and active carbons-oxygen sensors prepared from a tropical tree wood. *Carbon* 2005, **43**: 2152–2159.

[17] Hemanth J. Quartz (SiO_{2p}) reinforced chilled metal matrix composite (CMMC) for automotive applications. *Mater Des* 2009, **30**: 323–329.

[18] Xi JB, Zhou EZ, Liu YJ, *et al*. Wood-based straightway channel structure for high performance microwave absorption. *Carbon* 2017, **124**: 492–498.

[19] Wang SY, Hung CP. Electromagnetic shielding efficiency of the electric field of charcoal from six wood species. *J Wood Sci* 2003, **49**: 450–454.

[20] Wang LL, Tay BK, See KY, *et al*. Electromagnetic interference shielding effectiveness of carbon-based materials prepared by screen printing. *Carbon* 2009, **47**: 1905–1910.

[21] Du X, Zhang Z, Liu W, *et al*. Nanocellulose-based conductive materials and their emerging applications in energy devices—A review. *Nano Energy* 2017, **35**: 299–320.

[22] Barsoum MW. The M_N+1AX_N phases: A new class of solids. *Prog Solid State Chem* 2000, **28**: 201–281.

[23] Barsoum MW, El-Raghy T. The MAX phases: Unique new carbide and nitride materials. *Amer Scientist* 2001, **89**: 334–343.

[24] Mu Y, Zhou WC, Wan F, *et al*. High-temperature dielectric and electromagnetic interference shielding properties of SiC_f/SiC composites using Ti_3SiC_2 as inert filler. *Compos A*: *Appl Sci Manuf* 2015, **77**: 195–203.

[25] Onodera A, Terashima K, Urushihara T, *et al*. High-pressure synthesis of diamond from phenolic resin. *J Mater Sci* 1997, **32**: 4309–4318.

[26] Robertson J. Diamond-like amorphous carbon. *Mater Sci Eng*: *R*: *Rep* 2002, **37**: 129–281.

[27] Presser V, Naguib M, Chaput L, *et al*. First-order Raman scattering of the max phases: Ti_2AlN, Ti_2AlC_0.5N0.5, Ti_2AlC, $(Ti_{0.5}V_{0.5})_2AlC$, V_2AlC, Ti_3AlC_2, and Ti_3GeC_2. *J Raman Spectrosc* 2012, **43**: 168–172.

[28] Wang JY, Zhou YC, Lin ZJ, *et al*. Raman active phonon modes and heat capacities of Ti_2AlC and Cr_2AlC ceramics: First-principles and experimental investigations. *Appl Phys Lett* 2005, **86**: 101902.

[29] Stamm AJ. Three methods of studying capillary structure as applied to wood. *Physics* 1931, **1**: 116–128.

[30] Kang W, Chung WY. Liquid water diffusivity of wood from the capillary pressure-moisture relation. *J Wood Sci* 2009, **55**: 91–99.

[31] Bueche F. Electrical resistivity of conducting particles in an insulating matrix. *J Appl Phys* 1972, **43**: 4837–4838.

[32] Zeng S, Li X, Li M, *et al*. Flexible PVDF/CNTs/Ni@CNTs composite films possessing excellent electromagnetic interference shielding and mechanical properties under heat treatment. *Carbon* 2019, **155**: 34–43.

[33] Zhao B, Wang S, Zhao C, *et al*. Synergism between carbon materials and Ni chains in flexible poly(vinylidene fluoride) composite films with high heat dissipation to improve electromagnetic shielding properties. *Carbon* 2018, **127**: 469–478.

[34] Khazaei M, Arai M, Sasaki T, *et al*. Novel electronic and magnetic properties of two-dimensional transition metal carbides and nitrides. *Adv Funct Mater* 2013, **23**: 2185–2192.

[35] Shui W, Li J, Wang H, *et al*. $Ti_3C_2T_x$ MXene sponge composite as broadband terahertz absorber. *Adv Optical Mater* 2020, **8**: 2001120.

[36] Liu H, Wu S, You C, *et al*. Recent progress in morphological

engineering of carbon materials for electromagnetic interference shielding. *Carbon* 2021, **172**: 569–596.